# Supplementary Material for
# "Topology from Decoherence"

Alexandre Chaduteau,[1] Derek K. K. Lee,[1] Frank Schindler,[1] and Abhinav Prem[2]

[1] *Blackett Laboratory, Imperial College London, London SW7 2AZ, United Kingdom*
[2] *Physics Program, Bard College, 30 Campus Road, Annandale-on-Hudson, New York 12504, USA*

## CONTENTS

I. Lindbladians with quadratic jump operators 1
  A. Mapping $\mathcal{C}$ eigenmodes to $\mathcal{L}$ eigenmodes 2
  B. The Lindbladian skin effect remains a polynomial problem for quadratic jumps 4

II. Momentum space version of $\mathcal{C}$ 4

III. Decoherence-induced skin effect 6
  A. Explicit matrices 6
  B. Explaining the spectrum 7
  C. Analytical solutions to the eigenvalue equation 8
  D. Dynamical consequences 12

References 13

## I. LINDBLADIANS WITH QUADRATIC JUMP OPERATORS

Consider a density operator $\rho$ describing the state of a quantum system. For example, if the system is in a pure state described by $|\psi\rangle$, then $\rho = |\psi\rangle\langle\psi|$. With this definition, the Lindblad equation [1–4] is a dynamical equation for the density matrix that can be derived under a series of assumptions, the most prominent being the Born approximation, Markovianity, and the rotating-wave approximation [4]. It can be expressed as

$$\mathrm{i}\frac{\mathrm{d}\rho}{\mathrm{d}\tau} := \mathcal{L}(\rho) = [H,\rho] + \mathrm{i}\sum_m \left[K_m\rho K_m^\dagger - \frac{1}{2}\left\{K_m^\dagger K_m, \rho\right\}\right], \tag{1}$$

where $H$ is a Hermitian Hamiltonian and $K_m$ are "jump operators", which are operators on Fock space that describe interactions between the system and the environment. For our purposes, studying one-dimensional systems (with $N$ lattice sites), these jumps are labelled by an integer $m$, and there can be any number[1] of such jumps [4]. When all jumps are zero, we recover Schrödinger/von Neumann dynamics for closed quantum systems. Note that we adopt the convention whereby decay frequencies are directly incorporated in the definition of the jump operators.

In the case of quadratic Hermitian jump operators $K_m = K_m^\dagger$, the extra dissipative term becomes

$$\mathcal{L}_K(\rho) := \mathrm{i}\sum_m \left(K_m\rho K_m^\dagger - \frac{1}{2}\{K_m^\dagger K_m, \rho\}\right) = -\frac{\mathrm{i}}{2}\sum_m \left[K_m, [K_m, \rho]\right]. \tag{2}$$

With these quadratic jump operators, an initial Gaussian state will become non-Gaussian under time evolution. As in the main text, we study fermions $c_i, c_i^\dagger$ obeying canonical anti-commutation relations

[1] Although in the model we present here, we have as many jumps as lattice sites, i.e. $m \in \{1, \dots N\}$.

$\{c_i^\dagger, c_j\} = \delta_{ij},\ \{c_i, c_j\} = 0$. Let us consider the case of particle-number-conserving Hamiltonian and Hermitian quadratic jumps

$$
\begin{aligned}
H &= \sum_{i,j=1}^{N} \mathcal{H}_{ij} c_i^\dagger c_j, \\
K_m &= \sum_{i,j=1}^{N} (\mathcal{K}_m)_{ij} c_i^\dagger c_j,
\end{aligned}
\tag{3}
$$

where the matrices $\mathcal{H}_{ij}$ and $(\mathcal{K}_m)_{ij}$ are all Hermitian in $i, j$. One can obtain the equation of motion for the correlation matrix $C_{ij} = \langle c_i^\dagger c_j \rangle$ via $\frac{\mathrm{d}C_{ij}}{\mathrm{d}\tau} = \mathrm{Tr}(\dot{\rho} c_i^\dagger c_j) = -\mathrm{i}\mathrm{Tr}(\mathcal{L}(\rho) c_i^\dagger c_j)$ as

$$
\frac{\mathrm{d}C}{\mathrm{d}\tau} = \mathrm{i}\Theta^* \cdot C - C \cdot \mathrm{i}\Theta^T + \sum_m \mathcal{K}_m^T \cdot C \cdot \mathcal{K}_m^T, \tag{4}
$$

where we defined the $N \times N$ matrix

$$
\Theta_{ij} := \mathcal{H}_{ij} - \frac{\mathrm{i}}{2} \sum_m (\mathcal{K}_m^2)_{ij}. \tag{5}
$$

In Eq. (4), the first and second terms (which are Hermitian conjugates of each other) are responsible for coherent hopping in the chain. The new term $\sum_m \mathcal{K}_m^T \cdot C \cdot \mathcal{K}_m^T$ can be seen as an additional “interaction” term.

The equation of motion for the correlation matrix [Eq. (4)] itself takes the form of a Lindbladian. Vectorizing $C = \sum_{ij} C_{ij} |i\rangle \langle j|$ to $|C\rangle = \sum_{ij} C_{ij} |i\rangle \otimes |j\rangle$ gives

$$
\mathrm{i}\,|\dot{C}\rangle := \hat{\mathcal{C}}\,|C\rangle = \left[\Theta \otimes \mathbb{1} - \mathbb{1} \otimes \Theta^* + \mathrm{i} \sum_m \mathcal{K}_m \otimes \mathcal{K}_m^T\right] |C\rangle\,. \tag{6}
$$

The quadratic terms, some of which are inside $\Theta$, can altogether be written as $-\frac{\mathrm{i}}{2}\sum_m (\mathcal{K}_m \otimes \mathbb{1} - \mathbb{1} \otimes \mathcal{K}_m^T)^2$. Per the main text, $\hat{\mathcal{C}}$ is a $N^2 \times N^2$ matrix. Assuming it is invertible, Eq. (6) is formally solved by

$$
|C(\tau)\rangle = e^{-\mathrm{i}\hat{\mathcal{C}}\tau}\,|C(0)\rangle\,. \tag{7}
$$

The steady state's correlation matrix corresponds to $|\dot{C}\rangle = 0$ and is proportional to the identity in our case [5, 6]. Generically, $\hat{\mathcal{C}}$ is non-Hermitian and can be non-diagonalizable. Its size is quadratic in $N$, allowing to solve for dynamics of quadratic observables for much larger systems than by explicit diagonalisation of $\mathcal{L}$.

### A. Mapping $\mathcal{C}$ eigenmodes to $\mathcal{L}$ eigenmodes

We first construct single-particle eigenmodes of $\mathcal{L}$ from those of $\Theta$. From the adjoint action of the Lindbladian, one can obtain

$$
\begin{aligned}
\mathcal{L}^\dagger c_i &= -\sum_j \Theta_{ij} c_j, \\
\mathcal{L}^\dagger c_i^\dagger &= -\sum_j c_j^\dagger (\Theta^\dagger)_{ji}.
\end{aligned}
\tag{8}
$$

If we enforce translational invariance via $(\mathcal{K}_m)_{ij} = (\mathcal{K}_{m+1})_{i+1,j+1}$, then $\sum_m (\mathcal{K}_m^2)_{i+1,j+1} = \sum_{u=m-1} (\mathcal{K}_u^2)_{i,j} = \sum_m (\mathcal{K}_m^2)_{i,j}$. Assuming translational invariance of the Hamiltonian via $\mathcal{H}_{i+1,j+1} = \mathcal{H}_{ij}$, we have $\Theta_{ij} = \Theta_{i+1,j+1}$ as well.

Consider a left eigenvector $|L_a\rangle$ of $\Theta$, with components written $L_i^a$. Then the operator $X_a = \sum_i L_i^a c_i$ (and its dagger counterpart) is a right eigenmode of $\mathcal{L}^\dagger$, i.e. a left eigenmode of the Lindbladian. This reconstructs

$2N$ of the $4^N$ eigenmodes of the Lindbladian. Next, let us establish the relation between eigenvectors of $\hat{\mathcal{C}}$ and those of $\mathcal{L}$. Using Eq. (2), by methods in Ref. 7, we obtain

$$\mathcal{L}_K^\dagger Y = +\frac{\mathrm{i}}{2}\sum_m [K_m, [K_m, Y]]\,. \tag{9}$$

Using

$$\left[c_i^\dagger c_j, c_k^\dagger c_l\right] = \delta_{jk} c_i^\dagger c_l - \delta_{il} c_k^\dagger c_j \tag{10}$$

twice, we obtain

$$\mathcal{L}_K^\dagger c_i^\dagger c_j = \frac{\mathrm{i}}{2}\sum_{ml}\left[(\mathcal{K}_m^2)_{li} c_l^\dagger c_j + (\mathcal{K}_m^2)_{jl} c_i^\dagger c_l\right] - \mathrm{i}\sum_{mlk}(\mathcal{K}_m)_{li}(\mathcal{K}_m)_{jk} c_l^\dagger c_k. \tag{11}$$

Then the total adjoint action is

$$\begin{aligned}\mathcal{L}^\dagger c_i^\dagger c_j &= \sum_l\left[\left(\mathcal{H}_{il}^* + \frac{\mathrm{i}}{2}\sum_m(\mathcal{K}_m^2)_{li}\right) c_l^\dagger c_j + \left(-\mathcal{H}_{jl} + \frac{\mathrm{i}}{2}\sum_m(\mathcal{K}_m^2)_{jl}\right) c_i^\dagger c_l\right] \\ &\quad - \mathrm{i}\sum_{mlk}(\mathcal{K}_m)_{li}(\mathcal{K}_m)_{jk} c_l^\dagger c_k \\ &= \sum_l\left[\Theta_{il}^* c_l^\dagger c_j - c_i^\dagger c_l \Theta_{lj}^T\right] - \mathrm{i}\sum_{mlk}(\mathcal{K}_m)_{il}^T c_l^\dagger c_k (\mathcal{K}_m)_{kj}^T.\end{aligned} \tag{12}$$

An alternative way of deriving Eq. (4) starts from this action and uses the definition of the adjoint operator such that $\mathrm{Tr}\left[\mathcal{L}(\rho)X^\dagger\right] = \mathrm{Tr}\left[(\mathcal{L}^\dagger X)^\dagger \rho\right]$ for all operators $X$. Say the $\Theta$ eigenvector $|L_a\rangle$ has eigenvalue $T_a$. Then let $X_{ab} := \sum_{ij} L_i^{a*} L_j^b c_i^\dagger c_j$. We have

$$\mathcal{L}^\dagger X_{ab} = (T_a^* - T_b)X_{ab} - \mathrm{i}\sum_{mlkij}(\mathcal{K}_m)_{li}(\mathcal{K}_m)_{jk} L_i^{a*} L_j^b c_l^\dagger c_k. \tag{13}$$

Thus, single-particle left-eigenstates (those of $\Theta$) do not directly determine two-particle left-eigenstates due to the interaction term. Without it, we do reconstruct the postselected [4, 7] spectrum of $\hat{\mathcal{C}}$ completely, by which we mean the first two terms involving $\Theta$ and $\Theta^*$ in Eq. (6).

On the other hand, we can ask whether eigenvectors of $\hat{\mathcal{C}}$ determine those of $\mathcal{L}$. Indeed, let $\rho_C$ such that $\mathcal{L}(\rho_C) = \lambda_C \rho_C$. Then $C_{ij} := \mathrm{Tr}(\rho_C c_i^\dagger c_j)$ satisfies $\partial_\tau C_{ij} = -\mathrm{i}\mathrm{Tr}(\mathcal{L}(\rho_C)c_i^\dagger c_j) = -\mathrm{i}\lambda_C C_{ij}$. Vectorizing gives $\hat{\mathcal{C}}\,|C\rangle = \lambda_C\,|C\rangle$. We can also reverse-engineer a left eigenvector $X_C$ of $\mathcal{L}$ given a left eigenvector of $\hat{\mathcal{C}}$. For this, consider $\hat{\mathcal{C}}^\dagger(C) = \lambda C$. Then let $X_C = \frac{1}{2^{N-2}}\sum_{ij} C_{ji} c_i^\dagger c_j$, which satisfies

$$\mathrm{Tr}(X_C c_i^\dagger c_j) = \sum_{lk} C_{kl}(\delta_{ik}\delta_{lj} + \delta_{ij}\delta_{kl}) = C_{ij} + \delta_{ij}\mathrm{Tr}(C). \tag{14}$$

Using Eq.s (12) and (4) (and relabelling indices in the sums) we have

$$\begin{aligned}\mathcal{L}^\dagger X_C &= \frac{1}{2^{N-2}}\sum_{ijl}\left[\Theta_{li}^* C_{jl} - C_{li}\Theta_{jl}^T - \mathrm{i}\sum_m(\mathcal{K}_m^T)_{li} C_{ji} (K_m^T)_{jk}\right] c_i^\dagger c_j \\ &= \frac{1}{2^{N-2}}\sum_{ijl}\hat{\mathcal{C}}^\dagger(C)_{ji} c_i^\dagger c_j \\ &= \lambda X_C.\end{aligned} \tag{15}$$

Thus, left eigenmodes of $\hat{\mathcal{C}}$ correspond to left eigenmodes of $\mathcal{L}$. These correspond to the same correlation matrix, up to a factor proportional to the identity in Eq. (14). This is the two-particle analog of the fact that $\Theta$ left eigenvectors map to single-particle left eigenmodes of $\mathcal{L}$.

### B. The Lindbladian skin effect remains a polynomial problem for quadratic jumps

Consider an eigenmode $\rho_C$ of $\mathcal{L}$ with eigenvalue $\lambda_C$, so that under time evolution $\rho_C(\tau) = e^{-\mathrm{i}\lambda_C\tau}\rho_C$. We have the corresponding equation $\dot{C}_{ij}(\tau) = \mathrm{Tr}(\dot{\rho}_C(\tau)c_i^\dagger c_j) = -\mathrm{i}\lambda_C \mathrm{Tr}(\rho_C(\tau)c_i^\dagger c_j)$ i.e. $\dot{C}(\tau) = -\mathrm{i}\lambda_C C(\tau)$. So $C$ is an eigenvector of $\hat{\mathcal{C}}$ of eigenvalue $\lambda_C$. Yet the Lindbladian has $4^N$ eigenmodes but $\hat{\mathcal{C}}$ has only $N^2$; how is this possible? Clearly for all of these, the eigen-equation $\dot{C} = \lambda C$ must be satisfied. There are then three possibilities: (1) the eigenvalue $\lambda$ is zero, meaning the corresponding $C$ is a steady state solution; (2) $C = 0$; (3) for degenerate eigenvalues $\lambda_C$, we can also have linearly dependent $C$, which is a specific constrained case that we do not consider here. Thus, *for any Lindbladian whose steady state degeneracy does not scale exponentially with system size, and for which the correlation matrix equation of motion closes, we have at most $O(N^2)$ eigenmodes of $\mathcal{L}$ that have non-zero correlation matrix.* This directly implies that solving for skin effects is a polynomial ($\mathcal{O}(N^2)$) problem.

## II. MOMENTUM SPACE VERSION OF $\mathcal{C}$

As explained in Sec. I A, translational invariance of $\mathcal{H}$ and $\mathcal{K}_m$ implies that $\Theta$ is translationally invariant i.e. $\Theta_{i,j} = \Theta_{i+1,j+1}$, or in other words, $\Theta_{i,j} = \Theta_{i-j,0}$. Let us write the equation of motion for the correlation matrix as $\mathrm{i}\,|\dot{C}\rangle_{ij} = \sum_{l,n} \mathcal{C}_{ij,ln}\,|C\rangle_{ln}$, which from Eq. (4) requires

$$\mathcal{C}_{ij,ln} = \delta_{il}\Theta_{jn} - \Theta^*_{il}\delta_{jn} + \mathrm{i}\sum_m (\mathcal{K}_m)_{li}(\mathcal{K}_m)_{jn}. \tag{16}$$

Using the vectorization map $X_{ijln} = A_{il}B_{jn} \to \hat{X} = B \otimes A$, the superoperator $\hat{\mathcal{C}}$ takes the same form as before,

$$\hat{\mathcal{C}} = \Theta \otimes \mathbb{1} - \mathbb{1} \otimes \Theta^* + \mathrm{i}\sum_m \mathcal{K}_m \otimes \mathcal{K}_m^T, \tag{17}$$

where $\mathbb{1}$ represents the identity operator and $\otimes$ denotes a Krönecker product of matrices. Again, a few lines will show that $\mathcal{C}_{i,j,l,n} = \mathcal{C}_{i+1,j+1,l+1,n+1}$. This corresponds to saying that dynamics, which map a particle-hole pair's center of mass $(l+n)/2$ to another position $(i+j)/2$, does so regardless of the position on the lattice. The corresponding translation operator acts on the two-particle space via

$$\hat{T}\,|i,j\rangle := |i+1, j+1\rangle\,, \tag{18}$$

such that $\hat{T}\hat{\mathcal{C}}\hat{T}^{-1} = \hat{\mathcal{C}}$. We note that translational symmetry on ket indices only would give $\mathcal{C}_{i,j,l,n} = \mathcal{C}_{i+1,j+1,l,n}$; similarly, on bra indices only it would be $\mathcal{C}_{i,j,l,n} = \mathcal{C}_{i,j,l+1,n+1}$. The interaction term removes these as independent symmetries.

Now, let $a = j - i$ and $b = n - l$, so that $\mathcal{C}_{i,j,l,n} = \mathcal{C}_{i,i+a,l,l+b}$. Translational invariance allows shifting all indices by $-i$ to obtain $\mathcal{C}_{i,j,l,n} = \mathcal{C}_{0,a,l-i,l-i+b}$, which now only depends on three indices $a, b$, and $l - i$. The dynamical equation can be rewritten as

$$\mathrm{i}\dot{C}_{i,i+a} = \sum_{l,b} \mathcal{C}_{i,i+a,l,l+b}C_{l,l+b}. \tag{19}$$

We now introduce $k \in \frac{2\pi}{N}\mathbb{Z}$; multiplying both sides by $e^{\mathrm{i}ki}$ and summing over $k$ gives

$$\mathrm{i}\sum_i \dot{C}_{i,i+a}e^{\mathrm{i}ki} = \sum_{i,l,b} \mathcal{C}_{0,a,l-i,l-i+b}e^{\mathrm{i}k(i-l)}C_{l,l+b}e^{\mathrm{i}kl}. \tag{20}$$

We now define the left-hand side as $\mathrm{i}\sqrt{N}\dot{C}_{k,a}$. We also shift the $i$ sum at fixed $l$ to a sum over $i - l$ to obtain

$$\mathrm{i}\dot{C}_{k,a} = \sum_b \mathcal{C}_{ab}(k)C_{k,b}, \tag{21}$$

where (omitting the comma between indices $a$ and $b$)

$$\mathcal{C}_{ab}(k) := \sum_{i-l} \mathcal{C}_{0,a,l-i,l-i+b} e^{\mathrm{i}k(i-l)}. \tag{22}$$

This is the equivalent of the Bloch momentum-space matrix for tight-binding Hamiltonians. We can also rewrite the superoperator as

$$\begin{aligned}\hat{\mathcal{C}} &= \sum_{i,j,l,n} \mathcal{C}_{ijln}(|i\rangle\langle l|) \otimes (|j\rangle\langle n|) \\ &= \sum_{i,l,a,b} \mathcal{C}_{0,a,l-i,l-i+b} |i, i+a\rangle \langle l, l+b| \\ &= \frac{1}{N} \sum_{i,l,a,b,k} \mathcal{C}_{ab}(k) e^{\mathrm{i}k(l-i)} |i, i+a\rangle \langle l, l+b| .\end{aligned} \tag{23}$$

We now define $|k,a\rangle = \frac{1}{\sqrt{N}} \sum_i e^{-\mathrm{i}ki} |i, i+a\rangle$. These are eigenvectors of $\hat{T}$ as $\hat{T}|k,a\rangle = e^{\mathrm{i}k}|k,a\rangle$. By the usual route to the momentum-space Bloch Hamiltonian, we obtain

$$\hat{\mathcal{C}} = \sum_{a,b,k} \mathcal{C}_{ab}(k) |k,a\rangle \langle k,b| . \tag{24}$$

Plugging in the explicit form in Eq. (16), we obtain

$$\mathcal{C}_{ab}(k) = \Theta_{ab} - \Theta^*_{ba} e^{\mathrm{i}k(b-a)} + \mathrm{i} \sum_{i-l} \sum_m (\mathcal{K}_m)_{li} (\mathcal{K}_m)^*_{l+b,i+a} e^{\mathrm{i}k(i-l)}. \tag{25}$$

One issue is that this Bloch matrix's size scales with system size $N$. A similar case arises in Ref. [8]; in their case, assuming finite-range jumps, one can truncate this matrix to a finite size, independent of $N$. This is not true in our case due to the terms involving $\mathbb{1}$. In other words, the continuous part of the spectrum has infinitely many eigenvalues at each $k$ in the thermodynamic limit. On the other hand, the discrete part of the spectrum, which is where point-gap topology can occur [see main text], has finitely many eigenvalues at each $k$. The postselected part of $\hat{\mathcal{C}}$, which generates the continuum, has a second translational invariance in $b-a$. This corresponds to independent translational symmetries on ket/bra layers. As a result, the postelected part actually has a second momentum label $\kappa$. Explicitly, we write

$$\mathcal{C}^{\mathrm{post}}_{ab}(k) = \Theta_{ab} - \Theta^*_{ba} e^{\mathrm{i}k(b-a)}. \tag{26}$$

Since $\Theta$ is translationally invariant, we have the second translational symmetry $\hat{\tau}$ such that

$$\hat{\tau}\hat{\mathcal{C}}\hat{\tau}^{-1} = \hat{\mathcal{C}}, \tag{27}$$

associated with translational invariance of kets/bras independently. Letting $|k,\kappa\rangle = \frac{1}{\sqrt{N}} \sum_a e^{\mathrm{i}\kappa a} |k,a\rangle$, a similar procedure to the above yields

$$\hat{\mathcal{C}}^{\mathrm{post}} = \sum_{k,\kappa} \mathcal{C}^{\mathrm{post}}(k,\kappa) |k,\kappa\rangle \langle k,\kappa| , \tag{28}$$

where using $d := b-a$

$$\mathcal{C}^{\mathrm{post}}(k,\kappa) := \sum_d \mathcal{C}^{\mathrm{post}}_d(k) e^{\mathrm{i}\kappa d}. \tag{29}$$

Clearly then,

$$\mathcal{C}_{\mathrm{post}}(k,\kappa) = \Theta(k+\kappa) - \Theta(\kappa)^*. \tag{30}$$

Setting $\kappa = 0$ allows us to retrieve the winding of $\Theta(k)$. As for the previous truncation problem, we see that the part that cannot be truncated is precisely $\mathcal{C}^{\mathrm{post}}_{ab}(k)$, meaning the total $\mathcal{C}_{ab}(k)$ matrix has infinitely many identical blocks that repeat [see also Ref. [8]].

The SWAP symmetry of $\hat{\mathcal{C}}$ induces a symmetry on the Bloch matrix $\mathcal{C}_{ab}(k)$. This symmetry states that $\mathrm{i}\mathcal{C}_{ij,ln} = -\mathrm{i}\mathcal{C}^*_{ji,nl}$, which can be explicitly checked on Eq. (16). Then, we have

$$\begin{aligned}\mathcal{C}^*_{ab}(k) &= \sum_{i-l} \mathcal{C}^*_{i,j,l,n} e^{\mathrm{i}k(l-i)} \\ &= -\sum_{i-l} \mathcal{C}_{j,i,n,l} e^{\mathrm{i}k(l-i)} \\ &= -\sum_{l-i} \mathcal{C}_{0,-a,n-j,-b+n-j} e^{\mathrm{i}k(n-j+a-b)},\end{aligned} \tag{31}$$

where we used translational invariance to shift indices by $-j$. The sum index is $i-l$; when fixing $a, b$, this corresponds to summing over $j-n$. Thus

$$\begin{aligned}\mathcal{C}^*_{ab}(k) e^{\mathrm{i}k(b-a)} &= -\sum_{j-n} \mathcal{C}_{0,-a,n-j,-b+n-j} e^{\mathrm{i}k(n-j)} \\ &= -\mathcal{C}_{-a,-b}(-k),\end{aligned} \tag{32}$$

as in the main text.

## III. DECOHERENCE-INDUCED SKIN EFFECT

We now consider the following model:

$$\begin{aligned}H &= t \sum_{m=1}^{N} (c^\dagger_{m+1} c_m + \text{h.c.}), \\ K_m &= A c^\dagger_m c_m + \mathrm{i}B(c^\dagger_m c_{m+1} - c^\dagger_{m+1} c_m),\end{aligned} \tag{33}$$

where $t, A, B$ are all real parameters. Periodic boundary conditions (PBC) are implemented via $c_1 \equiv c_{N+1}$. The $B$ terms are the nearest-neighbor current operator, and the integer $m$ runs from 1 to $N$. The open-boundary counterpart of this model uses the last jump $K_N = A c^\dagger_N c_N$.

### A. Explicit matrices

In PBC, we have

$$\sum_{m=1}^{N} \mathcal{K}_m = \begin{pmatrix} A & \mathrm{i}B & 0\dots \\ -\mathrm{i}B & A & \mathrm{i}B\dots \\ \dots & \ddots & \dots \end{pmatrix}, \tag{34}$$

which is translationally invariant. In addition,

$$\sum_m \mathcal{K}_m^2 = \begin{pmatrix} A^2+2B^2 & \mathrm{i}AB & 0\dots \\ -\mathrm{i}AB & A^2+2B^2 & \mathrm{i}AB\dots \\ \dots & \ddots & \dots \end{pmatrix}, \tag{35}$$

which is a nearest-neighbour hopping matrix. We thus have a a point-gapped $\Theta$, since

$$\Theta = \mathcal{H} - \frac{\mathrm{i}}{2}\sum_m \mathcal{K}_m^2 = \sum_m \left[\left(t + \frac{1}{2}AB\right)|m\rangle\langle m+1| + \left(t - \frac{1}{2}AB\right)|m+1\rangle\langle m|\right] - \frac{\mathrm{i}}{2}(A^2+2B^2)\mathbb{1}, \tag{36}$$

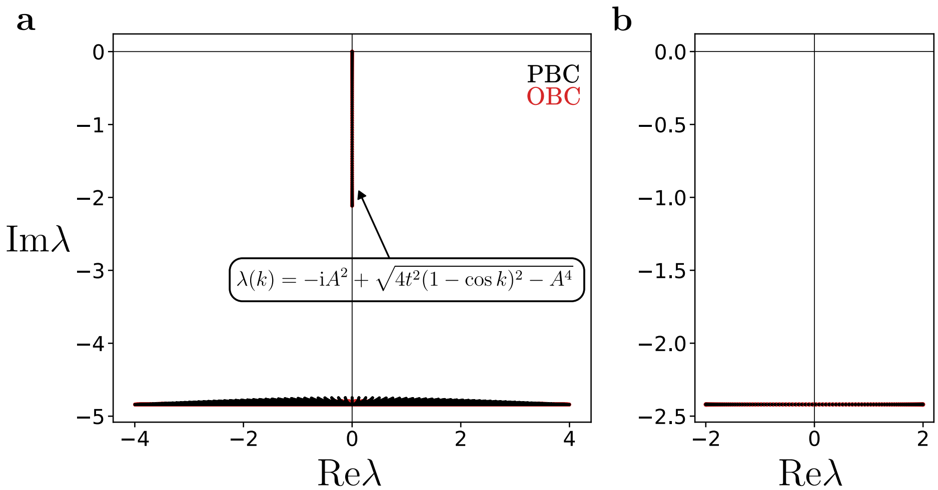


FIG. 1. Spectrum of the model without current measurements. **a.** Spectrum of $\hat{\mathcal{C}}$ for $t = 1, A = 2.2, B = 0$. When $B = 0$, the model obeys inversion symmetry [Eq. (39)] and the point gap is closed. Focusing on decohered-state eigenvalues, these match exactly the ones derived via Green's functions [Sec. III B]. **b.** Spectrum of $\Theta$, for which the point gap is closed as well, as expected from its hoppings involving $t \pm \frac{AB}{2}$.

and its Fourier components are $\Theta(k) = 2t\cos k - \frac{\mathrm{i}}{2}(A^2 + 2B^2 + 2AB\sin k)$. The corresponding matrix $\mathcal{C}_{ab}(k)$ [see Eq. (25)] is a tight-binding/Toeplitz PBC matrix. The postselected part is

$$\mathcal{C}^{\text{post}}_{ab}(k) = \begin{pmatrix} -\mathrm{i}(A^2+2B^2) & (t+g)-(t-g)e^{\mathrm{i}k} & 0 & \dots & (t-g)-(t+g)e^{-\mathrm{i}k} \\ (t-g)-(t+g)e^{-\mathrm{i}k} & -\mathrm{i}(A^2+2B^2) & (t+g)-(t-g)e^{\mathrm{i}k} & \dots & 0 \\ 0 & (t-g)-(t+g)e^{-\mathrm{i}k} & \dots & \dots & \dots \\ \vdots & & & & \\ (t+g)-(t-g)e^{\mathrm{i}k} & \dots & & & \end{pmatrix}, \tag{37}$$

where $g = \frac{1}{2}AB$. Its eigenvectors can be solved via the regular Bloch-wave ansatz, which will give the continuum's dispersion relation in $k$ and a second momentum label $\kappa$. As for the mixing term $\mathrm{i}\mathcal{C}^{\mathrm{Q}}_{ab}(k) := \mathcal{C}_{ab}(k) - \mathcal{C}^{\text{post}}_{ab}(k)$, we find

$$\mathcal{C}^{\mathrm{Q}}_{ab}(k) = \begin{pmatrix} A^2+2B^2\cos k & \mathrm{i}AB & 0 & \dots & -\mathrm{i}ABe^{-\mathrm{i}k} \\ -\mathrm{i}AB & 0 & 0 & \dots & -B^2e^{-\mathrm{i}k} \\ 0 & 0 & 0 & \dots & 0 \\ \vdots & \dots & \ddots & \dots & \vdots \\ \mathrm{i}ABe^{\mathrm{i}k} & -B^2e^{\mathrm{i}k} & 0 & \dots & 0 \end{pmatrix}, \tag{38}$$

which clearly does not have the additional translational symmetry of the postselected part [see Sec. II].

The point gap in $\Theta$ implies a non-Hermitian skin effect of single-particle left eigenmodes $\rho_a = \sum_i L^a_i c_i$ (and its dagger counterpart) for $L^a$ a left eigenmode of $\Theta$. This does not directly correspond to a skin effect in the two-point observables $\langle c_i^\dagger c_j \rangle$ due to the mixing term of $\hat{\mathcal{C}}$. When turning off the mixing term, the decohered point gap of $\hat{\mathcal{C}}$ disappears, implying that it is a purely "jump-induced" effect; it disappears upon postselection.

### B. Explaining the spectrum

Let us explain aspects of the spectrum [Fig. 1 of the main text]. Firstly, the mirror symmetry about the imaginary axis is due to the fact that eigenmodes come in conjugate pairs: $\mathcal{L}(\rho) = \lambda\rho \implies \mathcal{L}\rho^\dagger = -\lambda^*\rho^\dagger$. These eigenmodes are not Hermitian if their eigenvalue is not purely imaginary, and they are also traceless by trace-preservation. Secondly, the continuum is understood simply from the two momentum labels of $\mathcal{C}^{\text{post}}_{ab}(k)$ [see Eq. (26)]; expressing its solutions as Bloch waves reproduces the same spectrum. Thirdly, for $B = 0$, our model admits inversion symmetry, which maps site $m$ to site $-m$ up to an affine shift defining the inversion center. Ignoring that affine term, the corresponding symmetry is $\mathcal{C}_{i,j,l,n} = -\mathcal{C}_{-i,-j,-l,-n}$. Using Eq. (22), this implies

$$\begin{aligned}\mathcal{C}_{ab}(k) &= \sum_{i-l} \mathcal{C}_{0,-a,i-l,i-l-b} e^{\mathrm{i}k(i-l)} \\ &= \sum_{l-i} \mathcal{C}_{0,-a,i-l,i-l-b} e^{-\mathrm{i}k(l-i)} \\ &= \mathcal{C}_{-a,-b}(-k).\end{aligned} \tag{39}$$

Then, if $\lambda(k)$ is an eigenvalue, so is $\lambda(-k)$. Combining this with the SWAP symmetry implies pairs $\{\lambda(k), -\lambda^*(k)\}$. The continuum indeed comes in such pairs, at opposite real values and equal imaginary values. For decohered states, there can only be a single eigenvalue at momentum $k$. This forces $\lambda(k) = -\lambda^*(k)$ i.e. purely imaginary decohered-state eigenvalues.

Let us focus on the decohered band. The perturbation in $\mathcal{C}^{\text{Q}}_{ab}(k)$ for $B = 0$ is simple enough to allow analytical treatment. This can be treated as a bound state problem, akin to the Cooper instability problem [9]. In 1D, the density of states diverges near the bottom of the energy band, so there is a bound/decohered state for any nonzero perturbation strength. Assuming non-Hermiticity does not change the reasoning in Chapter 6 of Ref. [9], Green's function methods analytically give the decohered-state eigenvalues as

$$\lambda(k) = -\mathrm{i}A^2 \pm \sqrt{4t^2(1-\cos k)^2 - A^4}. \tag{40}$$

The Green's function method used is nonperturbative and gives a solution to all orders, so it is also true for $A > t$, as in our case. Expanding the above in $t/A$, we have

$$\begin{aligned}\lambda(k) &= -\mathrm{i}A^2 \pm \mathrm{i}A^2\sqrt{1 - \frac{4t^2(1-\cos k)^2}{A^4}} \\ &= -\mathrm{i}A^2 \pm \mathrm{i}A^2\left[1 - \frac{2t^2(1-\cos k)^2}{A^4}\right].\end{aligned} \tag{41}$$

From this we see two branches, one near the origin and one near $-2\mathrm{i}A^2$, the latter of which we discard. These eigenvalues are purely imaginary, as expected from inversion symmetry. The decohered band width scales with $t^2/A^2$. We plot an example of this spectrum in Fig. 1.

Crucially, perturbing with $B$ breaks the inversion symmetry of Eq. (39). Decohered-state eigenvalues are no longer required to satisfy $\lambda(k) = -\lambda^*(-k)$; in particular they can have a non-zero real part. This opens up the point gap, which is symmetric in $k$, by the SWAP symmetry of $\hat{\mathcal{C}}$.

### C. Analytical solutions to the eigenvalue equation

One can explicitly solve $\hat{\mathcal{C}}\,|C\rangle = \lambda\,|C\rangle$ [see Eq. (6)] for the model Eq. (33). Let us define $n_i = C_{ii}$, $l_i = C_{i,i+1}$, $r_i = C_{i+1,i}$. It is easiest to do it from the equation of motion rather than vectorizing; we obtain

$$\begin{aligned}(\lambda + 2\mathrm{i}c - \mathrm{i}A^2)n_i &= \mathrm{i}B^2(n_{i+1} + n_{i-1}) + (t-g)(r_{i-1} - l_{i-1}) + (t-g)(l_i - r_i), \\ (\lambda + 2\mathrm{i}c)r_i &= -(t+g)n_i + (t+g)n_{i+1} - \mathrm{i}B^2 l_i - (t+g)C_{i+2,i} + (t-g)C_{i+1,i-1}, \\ (\lambda + 2\mathrm{i}c)l_i &= (t+g)n_i - (t+g)n_{i+1} - \mathrm{i}B^2 r_i + (t+g)C_{i,i+2} - (t-g)C_{i-1,i+1}, \\ (\lambda + 2\mathrm{i}c)C_{i,i+2} &= (t+g)\left[C_{i,i+3} - C_{i+1,i+2}\right] + (t-g)\left[l_i - C_{i-1,i+2}\right], \\ (\lambda + 2\mathrm{i}c)C_{i+2,i} &= (t+g)\left[C_{i+2,i+1} - C_{i+3,i}\right] + (t-g)\left[C_{i+2,i-1} - r_i\right], \\ &\dots\end{aligned} \tag{42}$$

for all bulk $i = 2, \dots N-1$. Boundary equations can similarly be obtained. However, we are interested in the localization scaling, so it suffices to solve these bulk equations. Boundary conditions will simply dictate how to appropriately superpose the solutions.

Only the density ($n_i$) and currents (involving $r_i$ and $l_i$) have terms coming from interactions. All $C_{ij}$ can be non-zero, though we expect their magnitude to decay with the relative index $j-i=a$. Let us now study solutions under different truncation orders.

*Zeroth order truncation*— To zeroth order, one can truncate by setting $C_{i,i+a}=0\ \forall|a|\geq 1$. This gives an imaginary reciprocal tight-binding hopping in the $n_i$, so there is no skin effect there. This matches numerics, where the most classical states (the ones nearest to the steady state in the decohered band) have the least localization (and they are essentially most similar to the $B=0$ case).

*First order truncation*— To first order, we truncate via $C_{i,i+a}=0\ \forall|a|\geq 2$. Let us also define $\Lambda=\lambda+2\mathrm{i}c$. Then equations (42) reduce to

$$\begin{aligned}(\Lambda-\mathrm{i}A^2)n_i &= \mathrm{i}B^2(n_{i+1}+n_{i-1})+(t-g)(r_{i-1}-l_{i-1}+l_i-r_i),\\ \Lambda r_i &= (t+g)(n_{i+1}-n_i)-\mathrm{i}B^2 l_i,\\ \Lambda l_i &= -(t+g)(n_{i+1}-n_i)-\mathrm{i}B^2 r_i.\end{aligned} \tag{43}$$

We now ansatz $C_{ij}=\phi_{j-i}z^{i+j}$, for $\phi_{j-i}$ and $z$ complex numbers. Then, in particular, $n_i=\phi_0 z^{2i}$, $l_i=\phi_1 z^{2i+1}$, $r_i=\phi_{-1}z^{2i+1}$. Plugging these into the above, we obtain

$$\begin{aligned}\left[\Lambda-\mathrm{i}A^2-\mathrm{i}B^2(z^2+z^{-2})\right]\phi_0 &= \phi_1(t-g)(z-z^{-1})-\phi_{-1}(t-g)(z-z^{-1}),\\ \Lambda\phi_{-1}z &= (t+g)\phi_0(z^2-1)-\mathrm{i}B^2\phi_1 z,\\ \Lambda\phi_1 z &= -(t+g)\phi_0(z^2-1)-\mathrm{i}B^2\phi_{-1}z.\end{aligned} \tag{44}$$

Summing the last two equations gives

$$(\Lambda+\mathrm{i}B^2)(\phi_1+\phi_{-1})z=0, \tag{45}$$

meaning either $\lambda+2\mathrm{i}c+\mathrm{i}B^2=0$, or $z=0$, or $\phi_1=-\phi_{-1}$. Ignoring the first two cases, we obtain

$$\phi_1=\frac{1}{(\Lambda-\mathrm{i}B^2)z}(t+g)\phi_0(1-z^2). \tag{46}$$

Plugging this into the first equation, we obtain

$$\left[\Lambda-\mathrm{i}B^2\right]\left[\Lambda-\mathrm{i}A^2-\mathrm{i}B^2(z^2+z^{-2})\right]=2(t^2-g^2)\left[2-(z^2+z^{-2})\right]. \tag{47}$$

This is a quadratic equation in the coefficient $z^2$. While the explicit solution for $z^2$ can be obtained, it is more illuminating to expand near the steady state which is completely delocalized. We let $z^2=e^{\kappa}$. We have

$$\left[\lambda+\mathrm{i}(A^2+B^2)\right]\left[\lambda+\mathrm{i}B^2(2-(z^2+z^{-2}))\right]=2(t^2-g^2)\left[2-(z^2+z^{-2})\right]. \tag{48}$$

Expanding in $\kappa$ and rewriting $\lambda=-\mathrm{i}\Omega$, we obtain

$$\Omega^2-(A^2+B^2)\Omega+\Omega B^2\kappa^2-\left[(A^2+B^2)B^2+2(t^2-g^2)\right]\kappa^2+\ldots=0, \tag{49}$$

where dots indicate terms of order $\kappa^4$. Let us consider a solution $\kappa=\mathrm{i}\kappa_1\sqrt{\Omega}$. Expanding in leading orders of $\Omega$ gives

$$\Omega\left[-(A^2+B^2)+\Gamma\kappa_1^2\right]+\Omega^2\left[1-B^2\kappa_1^2\right]\approx 0, \tag{50}$$

where we defined $\Gamma=(A^2+B^2)B^2+2(t^2-g^2)$. Neglecting $\Omega^2$, we get

$$\kappa_1^2=\frac{A^2+B^2}{\Gamma}, \tag{51}$$

which is real. This gives purely oscillatory solutions with no localization length. While one could try other solutions / expand to higher orders, we can actually treat the more general case of a second-order truncation.

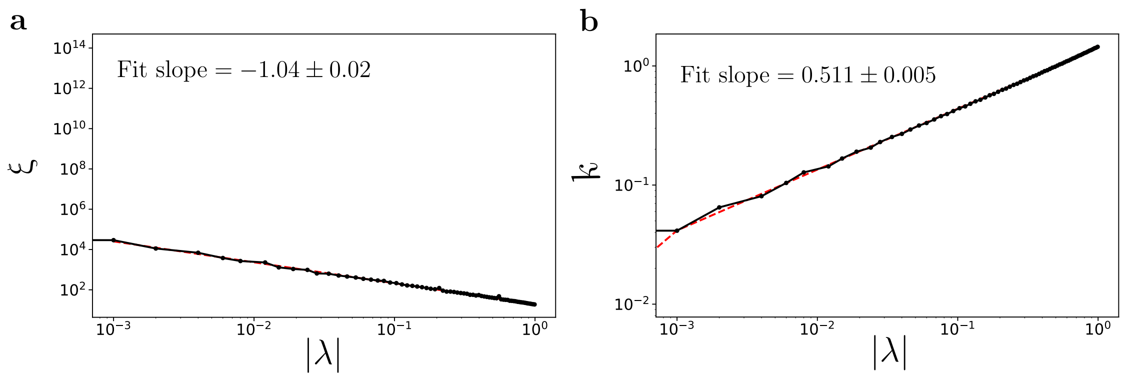


FIG. 2. Numerical fits of the localization length $\xi$ (a) and the oscillation wavevector $k$ (b) of decohered eigenmodes near the steady state in OBC. Parameters are the same as in Fig. 1 of the main text, i.e. $t = 1, A = 2.2, B = 0.5$. We fit the spatial profile of eigenmodes via the density $n_i$. The fit slopes roughly match the second-order predictions from Eq. (63).

*Second order truncation*— Let us now truncate to $C_{i,i+a} = 0 \ \forall |a| \geq 3$. With the same ansatz $C_{ij} = \phi_{j-i} z^{i+j}$, equations (42) become

$$\begin{aligned}
\left[\Lambda - \mathrm{i}A^2 - \mathrm{i}B^2(z^2 + z^{-2})\right] \phi_0 &= \phi_1(t-g)(z - z^{-1}) - \phi_{-1}(t-g)(z - z^{-1}), \\
\Lambda \phi_{-1} z &= \phi_0 (t+g)(z^2 - 1) - \mathrm{i}B^2 \phi_1 z - \phi_{-2}\left[(t+g)z^2 - (t-g)\right], \\
\Lambda \phi_1 z &= -\phi_0 (t+g)(z^2 - 1) - \mathrm{i}B^2 \phi_{-1} z + \phi_2\left[(t+g)z^2 - (t-g)\right], \\
\Lambda \phi_{-2} z^2 &= \phi_{-1} z\left[(t+g)z^2 - (t-g)\right], \\
\Lambda \phi_2 z^2 &= -\phi_1 z\left[(t+g)z^2 - (t-g)\right].
\end{aligned} \tag{52}$$

From this, defining $A_z = (t+g)z^2 - (t-g)$, we get

$$\begin{aligned}
\Lambda \phi_{-1} z &= \phi_0 (t+g)(z^2 - 1) - \mathrm{i}B^2 \phi_1 z - \frac{\phi_{-1} z A_z^2}{\Lambda z^2}, \\
\Lambda \phi_1 z &= -\phi_0 (t+g)(z^2 - 1) - \mathrm{i}B^2 \phi_{-1} z - \frac{\phi_1 z A_z^2}{\Lambda z^2}.
\end{aligned} \tag{53}$$

Computing their sum and difference gives, respectively,

$$\begin{aligned}
\Lambda(\phi_1 + \phi_{-1}) z &= -\mathrm{i}B^2(\phi_1 + \phi_{-1}) z - \frac{z A_z^2}{\Lambda z^2}(\phi_1 + \phi_{-1}), \\
\Lambda(\phi_1 - \phi_{-1}) z &= 2(t+g)(1 - z^2)\phi_0 + \mathrm{i}B^2(\phi_1 - \phi_{-1}) z - (\phi_1 - \phi_{-1})\frac{z A_z^2}{\Lambda z^2}.
\end{aligned} \tag{54}$$

From the first equation, either we have $\Lambda + \mathrm{i}B^2 + \frac{A_z^2}{\Lambda z^2} = 0$, or $\phi_1 = -\phi_{-1}$, or $z = 0$. From the second equation, we also have the case $\phi_1 = \phi_{-1}$, which requires either $t = -g$ (which we know numerically corresponds to a point gap closing) or $z = 1$, implying no localization. Let us focus on the case $\phi_1 = -\phi_{-1}$. The difference equation yields

$$\left[\Lambda - \mathrm{i}B^2 + \frac{A_z^2}{\Lambda z^2}\right] 2\phi_1 z = 2\phi_0 (t+g)(1 - z^2). \tag{55}$$

Plugging this into the first line of Eq. (52) gives

$$\left[\Lambda - \mathrm{i}B^2 + \frac{A_z^2}{\Lambda z^2}\right]\left[\Lambda - \mathrm{i}A^2 - \mathrm{i}B^2(z^2 + z^{-2})\right] = 2(t^2 - g^2)\left[2 - (z^2 + z^{-2})\right]. \tag{56}$$

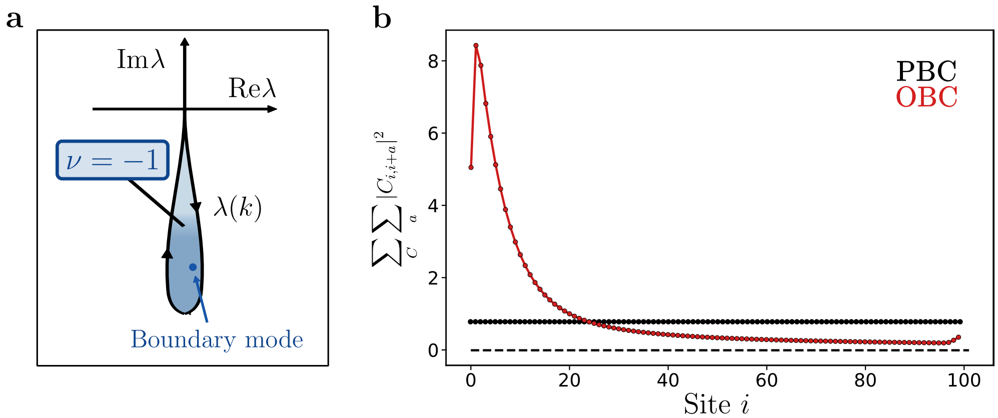


FIG. 3. **a.** Schematic of the point gap with winding reversed compared to the case considered in the main text [see Fig. 3 there]. Parameters used here are $t = 1, A = 2.7, B = 1.1, N = 100$. The winding direction of the spectrum of $\Theta$ remains the same as in the main text. **b.** Corresponding localization plot of decohered states, as per Fig. 3 of the main text. The localization reverses edges here. As a result, the asymmetric diffusion reverses direction. Thus, increasing $B$ can cause a reversal of the winding direction of $\hat{\mathcal{C}}$, while keeping that of $\Theta$ unchanged; this is an interaction-induced topological phase transition.

This is the same equation as Eq. (47) for the first-order truncation with an extra self-energy term. This no longer depends on any $\phi_a$ and allows us to derive a localization length. Again we rewrite $\lambda = -\mathrm{i}\Omega$ and let $z^2 = e^\kappa$. Expanding the two terms on the left-hand side in $\kappa$ separately gives

$$\begin{aligned} \left[\Lambda - \mathrm{i}A^2 - \mathrm{i}B^2(z^2 + z^{-2})\right] &= -\mathrm{i}(\Omega + B^2\kappa^2) + \dots, \\ \left[\Lambda - \mathrm{i}B^2 + \frac{A_z^2}{\Lambda z^2}\right] &= \mathrm{i}\left[\Gamma_0 - (\gamma_1 + \gamma_1') - (\gamma_1 - \gamma_1')\kappa - \frac{\gamma_1 + \gamma_1'}{2}\kappa^2 - \frac{\gamma_1 - \gamma_1'}{6}\kappa^3 + \dots\right], \end{aligned} \tag{57}$$

where the dots indicate higher orders of $\kappa$. We also defined $\Gamma_0 = A^2 + B^2 + 2\frac{t^2-g^2}{A^2+2B^2}$, $\gamma_1 = \frac{(t+g)^2}{A^2+2B^2}$, $\gamma_1' = \frac{(t-g)^2}{A^2+2B^2}$. Let also $\Gamma_1 = \gamma_1 - \gamma_1' = \frac{4tg}{A^2+2B^2}$, $\Gamma_1' = \gamma_1 + \gamma_1' = 2\frac{t^2+g^2}{A^2+2B^2}$. Plugging this into Eq. (56) gives the condition

$$(\Gamma_0 - \Gamma_1')\Omega - \Gamma_1\Omega\kappa - \frac{\Gamma_1'}{2}\Omega\kappa^2 + \Gamma_2\kappa^2 - B^2\Gamma_1\kappa^3 - \frac{\Gamma_1}{6}\Omega\kappa^3 + \dots = 0, \tag{58}$$

where we also defined $\Gamma_2 = (\Gamma_0 - \Gamma_1')B^2 + 2(t^2 - g^2)$. We can then approximate the solution as

$$\kappa \sim \kappa_0\Omega \pm i\kappa_1\sqrt{\Omega}. \tag{59}$$

Plugging this into Eq. (58), we get the consistency conditions (to leading order)

$$\kappa_1^2 = \frac{\Gamma_0 - \Gamma_1'}{\Gamma_2} = \frac{A^2 + B^2 - \frac{4g^2}{A^2+2B^2}}{(A^2 + B^2 - \frac{4g^2}{A^2+2B^2})B^2 + 2(t^2 - g^2)} \tag{60}$$

and to next order

$$\kappa_0 = \frac{\Gamma_1\Gamma_2 - B^2\Gamma_1(\Gamma_0 - \Gamma_1')}{2\Gamma_2^2} = \frac{\Gamma_1(t^2 - g^2)}{\Gamma_2^2}. \tag{61}$$

Note here that we need $\Gamma_0 - \Gamma_1' > 0$ for this to make sense; this is always true for real $A, B$ since

$$\begin{aligned} \Gamma_0 - \Gamma_1' &= A^2 + B^2 + 2\frac{t^2 - g^2}{A^2 + 2B^2} - 2\frac{t^2 + g^2}{A^2 + 2B^2} \\ &= \frac{A^4 + 2A^2B^2 + 2B^4}{A^2 + 2B^2} \geq 0. \end{aligned} \tag{62}$$

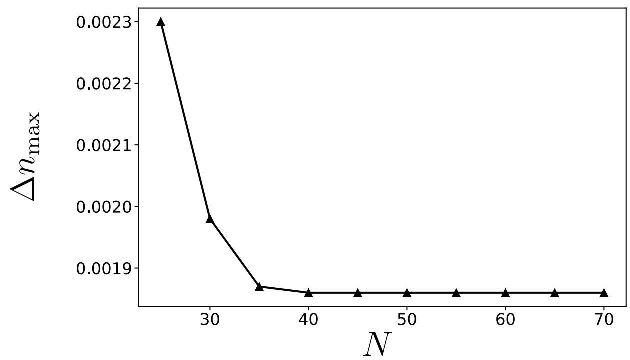


FIG. 4. Scaling of the maximum asymmetry $\Delta n_{\max} = n(\mu - 2\sigma) - n(\mu + 2\sigma)$, for $\mu$ the mean of the initial Gaussian correlation matrix perturbation and $\sigma$ its standard deviation. Here $\mu = \lfloor N/2 \rfloor$ with $N = 100$. Also, $\epsilon = 7$ in Eq. (65) and $\sigma = 5$, as in Fig. 2 of the main text. We obtain $\Delta n_{\max}$ by time-evolving the system at each $N$ and finding the time $\tau$ for which the asymmetry is maximal. We clearly see a convergence of $\Delta n_{\max}$ with increasing system size $N$, precluding its interpretation as a finite-size effect.

So the two relevant non-Bloch roots are

$$\boxed{\kappa_\pm \approx \frac{\Gamma_1(t^2 - g^2)}{\Gamma_2^2}\Omega \pm \mathrm{i}\sqrt{\frac{\Gamma_0 - \Gamma_1'}{\Gamma_2}}\sqrt{\Omega}}. \tag{63}$$

The imaginary part gives the long-wavelength oscillation, while the common real part gives the exponential skin profile. From this, we can now read off the localization length

$$\xi^{-1} = |\mathrm{Re}(\kappa)| = \left| \frac{\Gamma_1(t^2 - g^2)}{\Gamma_2^2} \right| |\lambda|. \tag{64}$$

This scaling matches a numerical fit, as shown in Fig. 2. In OBC, the eigenmodes lie on the imaginary axis, meaning their correlation matrix is Hermitian. This constrains the possible superpositions of the two solutions $\kappa_\pm$ here. As their real part is equal, fitting numerical eigenmodes to a single exponential does suffice to extract $\xi$. At $B = 0$, $\Gamma_1 = 0$ (since $g = AB/2$) and $\Gamma_2$ remains finite, so there is no localization, as expected. In addition, flipping the sign of $B$ flips the sign of $g$, which flips $\Gamma_1$, which dictates the side on which localization occurs. This also shows that the localization length diverges when $t = \pm g$. In that case, $\kappa_1^2 = 1$, so $\kappa \sim \mathrm{i}\sqrt{\Omega}$ still oscillates, which we verified numerically. Lastly, the fact that the localization plots [Fig. 3 here and also Fig. 3 of the main text] peak not at the edge but slightly before is likely an effect of the boundary conditions, which we do not consider here.

### D. Dynamical consequences

We now discuss the behavior of perturbations from the steady state. More precisely, we consider initial states described by correlation matrices

$$C(0) = C_S + \epsilon \cdot \delta C, \tag{65}$$

for $\epsilon > 0$ some small real parameter, and $\delta C$ some perturbation of choice. We will consider $\delta C$ that gives a Gaussian density profile located at the middle of the chain, with some spread $\sigma$.

As established in the main text, one dynamical consequence of the decohered point gap is asymmetric diffusion on a large timescale. A few sanity checks can be performed: firstly, this effect vanishes when $B = 0$. Secondly, diffusion is completely symmetric at the points $t = \pm g$, where the decohered point gap closes. Thirdly, the direction of asymmetry reverses with the winding direction of the point gap, as shown in Fig. 5(a). Fourthly, using only the postselected part $\hat{\mathcal{C}}^{\mathrm{post}}$ to time-evolve, this effect disappears and is replaced by asymmetric coherent hopping on a much shorter timescale, as shown in Fig. 5(b).

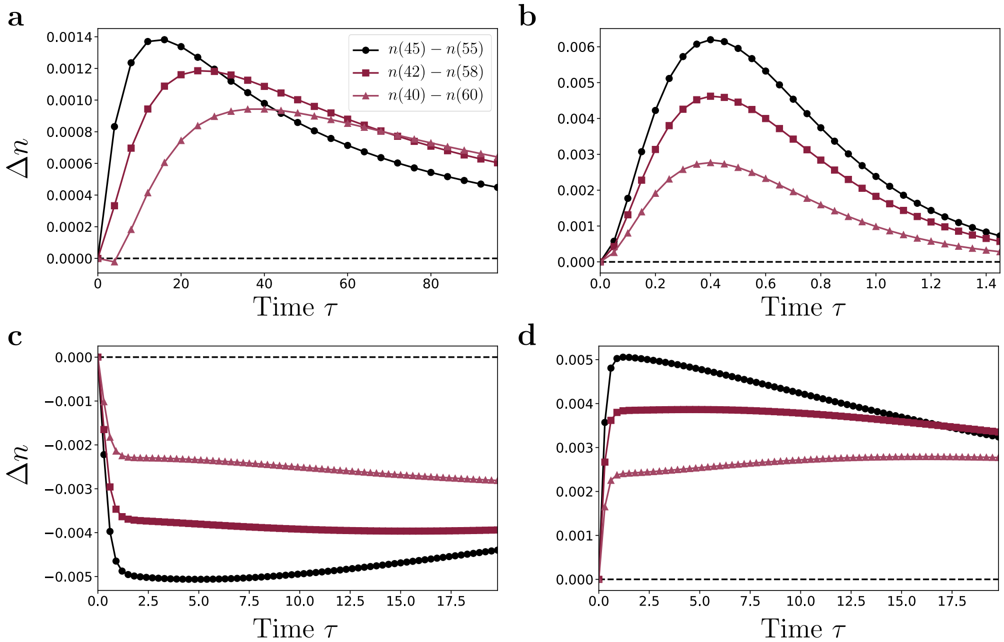


FIG. 5. **a.** Asymmetric diffusion for the case where the decohered point gap winds in the same way as $\Theta$, as in Fig. 3 (with the same parameters). Correspondingly, the asymmetric diffusion reverses direction compared to Fig. 2 of the main text. **b.** Postselected dynamics of the same initial perturbation for $N = 50$. The timescale is now much shorter, matching the larger magnitude of the decay rate of continuum eigenmodes. We observe non-reciprocal coherent hopping, as in a non-Hermitian Hamiltonian. **c.** Full dynamics (non-postselected) for a pure-state perturbation atop the steady-state [Eq. (67)] for the same parameters as in Fig. 2 of the main text. The long-lived asymmetric diffusion is the same, with short-lived initial peak explained by coherent hopping, as in panel c. **d.** Same as panel c but with the reverse-winding parameters as in Fig. 3.

We verified this for two different initial perturbations $\delta C$. The first is a diagonal matrix with Gaussian density distribution

$$\delta C_{ii} = e^{-(i-\mu)^2/(2\sigma^2)}, \tag{66}$$

centered mid-chain, i.e. $\mu = \lfloor N/2 \rfloor$. We also divide this by the maximum argument to normalize. The second is a pure Gaussian wavepacket, constructed from a pure state

$$|\psi\rangle = \sum_i e^{-(i-\mu)^2/(4\sigma^2)} |i\rangle\,, \tag{67}$$

where $i = 1, \dots N$. After normalizing this, we construct $\delta C = |\psi\rangle\langle\psi|$. This has the same density profile as the other initialization. However, this second initialization kind is not a diagonal correlation matrix and has higher purity. The only difference in their dynamics occurs initially, in the way they couple to continuum eigenmodes. After a few multiples of the continuum timescale, these both display the same qualitative asymmetric diffusion profile, which is near-classical.

We have also verified that dynamics under $\hat{\mathcal{C}}$ match that obtained from explicit diagonalization of the many-body $4^N \times 4^N$ Lindbladian superoperator for $N = 5$ fermions.

[1] G. Lindblad, Communications in Mathematical Physics **48**, 119 (1976).
[2] V. Gorini, A. Kossakowski, and E. C. G. Sudarshan, Journal of Mathematical Physics **17**, 821 (1976).
[3] A. J. Daley, Advances in Physics **63**, 77 (2014), https://doi.org/10.1080/00018732.2014.933502.
[4] H.-P. Breuer and F. Petruccione, *The theory of open quantum systems* (OUP Oxford, 2002).

[5] B. Horstmann, J. I. Cirac, and G. Giedke, Phys. Rev. A **87**, 012108 (2013).
[6] T. Barthel and Y. Zhang, Journal of Statistical Mechanics: Theory and Experiment **2022**, 113101 (2022).
[7] A. Chaduteau, D. K. K. Lee, and F. Schindler, Phys. Rev. Lett. **136**, 016603 (2026).
[8] M. Nakagawa and M. Ueda, Phys. Rev. X **15**, 021016 (2025).
[9] E. N. Economou, *Green's functions in quantum physics* (Springer, 2006).